



A novel optimal sensor placement software for supporting the development of monitoring systems in civil engineering structures

Simone Quarchioni¹ · Vanni Nicoletti¹ · Fabrizio Gara¹

Received: 15 July 2025 / Accepted: 10 January 2026
© The Author(s) 2026

Abstract

This paper proposes a new software for the Optimal Sensor Placement (OSP) featuring an intuitive graphical user interface that simplifies its use. The software automates OSP analyses, enhancing efficiency, reducing human error, and supporting the development of effective dynamic monitoring systems as a result. It incorporates five well-established OSP methods that allow users to explore the optimal number of sensors and their locations on a structure. Moreover, it accommodates both numerical and experimental data as input. Results are provided in both tabular and graphical format. It can be used in all types of structures, even though it was developed primarily for civil engineering applications. A key innovation of the proposed software is its ability to perform OSP analyses on multi-block, complex, and non-orthogonal buildings, increasing versatility. After a comprehensive description of the new software, its applicability and potentiality are shown through simple applications, as well as with real case studies.

Keywords Optimal sensor placement · OSP software · Structural health monitoring · Dynamic monitoring · Complex building geometry · Civil engineering structures

1 Introduction

Structural Health Monitoring (SHM) is crucial for both existing and new structures because it ensures safety, enhances durability, and reduces maintenance costs [1]. Key components of a SHM system include sensors, with both their type and strategic placement across the structure being essential. It is well-established that sensor networks with high spatial density enhance both the quantity and quality of monitoring information; however, a large number of sensors introduces challenges related to data storage, management, and costs [2]. In this context, Optimal Sensor Placement (OSP) strategies emerge as a crucial aspect, serving as a balance between the feasibility of SHM system development and the utility of the gathered information [3, 4]. The OSP in civil engineering structures enhances automated management by enabling real-time monitoring, predictive maintenance, and

smart response systems [5]. Strategically placed sensors ensure that critical areas are monitored, detecting damage early and reducing the need for on-site inspections. OSP also integrates with automated control systems, triggering safety measures during disasters and improving efficiency in large infrastructure networks [6]. By reducing costs, enhancing safety, and ensuring regulatory compliance, OSP enables a shift from reactive to proactive structural management with minimal human intervention. Moreover, for structures with intricate geometries, determining the optimal locations of sensors becomes a non-trivial task [7, 8]. Improper positioning of sensors can result in the generation of unreliable data, potentially causing significant changes in structural response to go unnoticed [9].

Many OSP methods have been proposed in the last few decades, initially focusing on aerospace applications [10] and later expanding to many fields [11]. For instance, OSP methods are developed to find the best sensor configuration for the monitoring of Reinforced Concrete (RC) complex structures, such as a vaulted roof [12] and an arch dam [13], steel towers [14, 15], bridges [16–18], and heritage masonry structures [19, 20]. Comprehensive review papers about the topic of OSP are available in the literature. For instance, the work of Yi et al. [21] presents an interesting review

✉ Vanni Nicoletti
v.nicoletti@univpm.it

¹ Department of Construction, Civil Engineering and Architecture (DICEA), Università Politecnica delle Marche, Ancona, Italy

collecting the available methodologies for OSP in civil engineering structures and infrastructures. A more detailed review about OSP methods with particular emphasis on available techniques based on vibration measurements is provided by Li et al. [22].

Although the importance of OSP in the context of SHM is widely acknowledged and numerous OSP methods exist, there are very few tools that enable this type of analysis to be conducted in a fully automated and user-friendly manner. Only few examples of OSP software are already available and they encompass a broad range of applications. For instance, Hart et al. [23] developed the first OSP toolkit called SPOT in 2007; however, this toolkit was created for specific applications concerning the development of drinking water contamination warning systems. In 2016 Arnesano et al. [24] proposed a software for the OSP, but still focused on a specific purpose, namely, to optimize temperature monitoring within buildings. In 2017 Klise et al. [25] released the Chama software, which is an adjourned and improved version of the SPOT software originally developed by Hart et al. in 2007. Although its functionality has expanded beyond the original version, Chama software remains applicable to the environmental monitoring sector. In 2019 Dong et al. [26] released a new sensor placement optimization tool that works considering three optimization methods: the greedy algorithm, the standard genetic algorithm, and a hybrid genetic algorithm. However, this software requires the schematization of many structural characteristics to be used, among which the node coordinates and connection relationships. For this reason, the applicability of this software is mainly suitable for users who want to develop their own OSP strategy with the support of a guided procedure provided by the software. Lastly, in 2023, Tang et al. [27] proposed a OSP toolkit (named OSPtk) to achieve cost-effective monitoring systems in critical industrial systems.

Concerning civil engineering structures, very few tools are currently available. In 2011, Yi and Gu [28] developed a new OSP strategy and created a Matlab toolbox with a Graphical User Interface (GUI) to make the OSP more accessible and easily usable to civil engineers. However, only one OSP method, based on a genetic algorithm, was implemented in this toolbox, and it was tested on a single case study, namely, the tall structure of the Guangzhou TV Tower in China. Several years later, in 2019, Wu et al. [29] proposed a software suitable for determining the optimal position of strain gauges and accelerometers on structures when monitoring systems are required. The software operated using only one OSP methodology, the fast messy genetic algorithm [30], and it was tested by considering a single case study involving a large-span cable-stayed bridge in India. Another OSP tool was proposed by Mahjoubi et al. [31] in 2020, working with the hypotrochoid spiral

optimization algorithm [32] as OSP method. This tool did not have a GUI and it was tested considering a single case study consisting in the tall Shanghai Tower in China.

The very low number of software already available and their limited functions convinced the authors about the importance to develop a new tool for the OSP purpose, with emphasis to the civil engineering field. To this aim, this paper proposes a new software for the OSP of civil engineering structures and infrastructures. The software is developed in Matlab environment and is equipped with a GUI that makes it easy and intuitive to be used, even for the user who has not experience in computer coding. This new software supports users to automatically perform OSP analyses, improving efficiency, reducing human error, and enabling the development of more effective dynamic monitoring systems. The software incorporates 5 well-established OSP methods from the literature and includes the calculation of metrics that allow the optimal number of sensors to be investigated as well. Moreover, differently from the majority of the software already existing, both numerical and experimental data can be uploaded and used as a basis for the analyses. Results are returned both in tabular form and through the display of figures clearly showing the position of the selected sensors over the structure. In addition, one of the original and fundamental strengths of this new software is its capability to perform OSP analyses simultaneously on multiple building blocks with complex geometries and various orientations, including non-orthogonal configurations.

The content of the paper is divided as follows: after a brief recall of the adopted OSP methods (Sect. 2), the novel software is presented and deeply described in Sect. 3, adding discussions and details about its use. Section 4 and Sect. 5 are devoted to prove the software efficiency and usefulness through simple numerical and real case study applications, respectively. Finally, Sect. 6 addresses the potentiality of the novel software in performing OSP analysis in building with complex geometry.

2 Brief recall of the adopted OSP methods

The goal of an OSP method in developing dynamic SHM systems is to individuate a minimal set of sensors (considering their locations and measurement directions) that allows the identification of vibration modes as linearly independent as possible, while preserving the maximum amount of modal information about the analysed structure. Generally, the number of sensors to be adopted is predetermined, often correlated with the available fundings, while the target modes to be considered and monitored are case- and purpose-dependent. To determine the optimal positions of sensors, a proper evaluation criterion is essential. Common

OSP methods allow the assessment, in one or more iterations, of the contribution of each candidate joint (or Degree Of Freedom - DOF) to the mode identifiability based on a specific metric, typically a numerical coefficient derived from the mode shape matrix.

In the presented software, 5 well-known OSP methods from the relevant literature have been implemented: Effective Independence (EI) [33], Information Entropy (IE) [34], Eigenvalue Vector Product (EVP) [35], Mode Shape Summation Plot (MSSP) [36], and Average Driving Point Residue (ADPR) [37]. The basics of these methods are briefly summarized below. For more details, the reader may refer to [38]. The EI method, widely recognized and utilized in structural engineering, is distinguished by its computational efficiency, as it avoids resource-intensive search techniques. It involves selecting target vibration modes for a structure and iteratively refining a candidate set of sensor locations or DOFs based on modal displacements. The process is guided by the Fisher information matrix which eliminates non-contributing DOFs. To begin, target vibration modes (k) and an initial set of candidate sensor locations (s) are chosen for the structure. The modal displacements of these candidates are organized in the Φ_s matrix (where rows are the s DOFs and columns are the k modes), and the procedure starts solving the eigenvalue equation:

$$[\mathbf{A}_0 - \lambda \mathbf{I}] \Psi = 0 \tag{1}$$

where the vectors Ψ represent k orthogonal directions and \mathbf{A}_0 is the Fisher information matrix, which can be expressed as:

$$\mathbf{A}_0 = \Phi_s^T \Phi_s \tag{2}$$

Then, the matrix \mathbf{F}_E is computed by the term-by-term matrix multiplication:

$$\mathbf{F}_E = [\Phi_s \Psi] \otimes [\Phi_s \Psi] \lambda^{-1} \tag{3}$$

Finally, the \mathbf{E}_D vector is calculated by summing the terms within each row of \mathbf{F}_E :

$$E_D = \left[\sum_{j=1}^k F_{E1,j}; \sum_{j=1}^k F_{E2,j}; \dots; \sum_{j=1}^k F_{Es,j} \right]^T \tag{4}$$

The i -th term in \mathbf{E}_D represents how much the i -th sensor location (or DOF) contributes to the linear independence of Φ_s . If $E_{D,i}$ equals 0, the sensor location provides no contribution, making the system unobservable from that position; if $E_{D,i}$ equals 1, retaining this sensor location in the final configuration is necessary to identify the target modes. This process is repeated iteratively by removing the i -th row of

the Φ_s matrix at each step which corresponds to the least contribution to the linear independence of the target vibration modes.

The IE method, an enhancement of EI, treats optimal sensor configuration as a discrete optimization problem, minimizing the objective function to provide insights into system parameter uncertainty. The objective function used is the Information Entropy (IE), with the discrete variables representing the number and positions of the sensors. The IE for a given sensor configuration is calculated using:

$$IE = \frac{1}{2} N_\theta \ln(2\pi) - \frac{1}{2} \ln \{ \det[\mathbf{A}_0(\mathbf{L})] \} \tag{5}$$

where N_θ is the number of DOFs and \mathbf{L} is a Boolean matrix that selects the DOFs within the Φ_s matrix. The method begins by including all the DOFs in Φ_s and then iteratively removes one sensor location at a time, prioritizing the position that causes the smallest increase in IE.

In contrast, the EVP method identifies optimal sensor locations in a single step by assessing the significance of the EVP coefficient of each DOF, thereby avoiding iterative procedures. This method focuses on maximizing the absolute product of row values in the modal partition matrix:

$$EVP_i = |\Phi_{i1}| \times |\Phi_{i2}| \times \dots \times |\Phi_{ik}| = \prod_{j=1}^k |\Phi_{ij}| \tag{6}$$

The MSSP method is similar to EVP but aims to maximize the absolute sum of modal displacements in each row of the modal partition matrix:

$$MSSP_i = |\Phi_{i1}| + |\Phi_{i2}| + \dots + |\Phi_{ik}| = \sum_{j=1}^k |\Phi_{ij}| \tag{7}$$

The ADPR method, another energy-based OSP approach, evaluates the mean contribution of each potential sensor location to mode shapes by considering the circular frequency of each vibration mode:

$$ADPR_i = \sum_{j=1}^k \frac{\Phi_{ij}^2}{\omega_j} \tag{8}$$

The first vibration modes are assumed more important than the higher ones (since the frequency increases with mode number), and the coordinates with the highest $ADPR_i$ are chosen as sensor locations.

The EI and IE methods offer the advantage of ensuring highly linear independence of the target modes, which supports reliable dynamic identification, while also being computationally efficient. However, they may select sensor locations with low energy content, resulting in a poor

signal-to-noise ratio and reduced accuracy in mode shape identification. Conversely, the EVP, MSSP, and ADPR methods prioritize locations with higher modal displacements, but their main limitation lies in the excessive weight assigned to the first vibration modes.

The effectiveness of the configurations obtained after the OSP procedure is quantitatively assessed using metrics, which are numerical coefficients that indicate the robustness of the sensor configuration for accurately identifying the mode shapes of the selected modes. Employing metrics facilitates a thorough evaluation of sensor configurations produced by various OSP methods, ensuring consistent and comparable coefficients across different approaches. In the software, two metrics are implemented: the Average Value of the off-diagonal terms of the AutoMAC Matrix (AVAM) and the Information Entropy Index (IEI). AVAM evaluates the linear independence of mode shapes, where lower values indicate better differentiation, ranging from 0 to 1. This metric is calculated with the following formula:

$$AVAM = \frac{\sum_i \sum_j (\mathbf{AutoMAC} - \mathbf{I})}{N} \quad (9)$$

where $\mathbf{AutoMAC}$ is the AutoMAC matrix calculated considering the selected DOFs, \mathbf{I} is the identity matrix, and N is the total number of the $k \times k$ AutoMAC matrix elements.

The IEI metric, a normalized form of the IE, seeks values close to 1, representing perfectly orthogonal mode shapes. It is defined by

$$IEI = \sqrt{\frac{\det \mathbf{A}_0(\mathbf{L}_{ref})}{\det \mathbf{A}_0(\mathbf{L})}} \quad (10)$$

where \mathbf{L}_{ref} refers to the full sensor configuration.

The metric evolution is of great support to evaluate how the performance of a sensor configuration in capturing mode shapes changes with the variation of the number of monitored DOFs. By tracking a metric as the number of final DOFs varies, the user can determine the optimal number of sensors needed to effectively capture the dynamic behaviour of a structure, together with their optimal positions.

3 Description of the novel OSP software

The OSP software proposed in this work is suitable for the determination of the appropriate number of sensors and their locations for the development of dynamic SHM systems of civil engineering structures and infrastructures. The software is created in Matlab environment and is equipped with a very intuitive GUI (Fig. 1, created using Matlab App Designer Version R2023b) that guides the user in developing the analyses. The software is released both as a Matlab application for Matlab users and as a standalone desktop application with the Matlab compiler. The latter only requires the installation of the free Matlab runtime.

Initially, data needed for the OSP procedure must be loaded. These data include mode shape displacements and frequencies of target modes. The software offers two data entry options: manual entry, by uploading tables in .xlsx file type, and automatic entry from SAP2000. The former enables the loading of both numerical and experimental data, allowing the software to be used for design or optimize SHM systems using numerical models or on-site measurements.

When the manual import procedure is selected, two tables prepared in files with standard layout (created in .xlsx format) have to be provided. The first table (Fig. 2a), called "Modal Displacements Input", collects information about the geometry of the structure (coordinates of all/selected joints in which the structure is discretized) and the modal displacements of these joints. The first two columns gather the name of joints and the anticlockwise angle between their local reference system with the global one. This angle is used for calculating modal displacements along the directions of the local reference systems, as well addressed in Sect. 6. From the 3rd to the 5th columns the geometrical coordinates of joints referring to a global 3D coordinate system (X, Y, and Z) are inserted. The other columns are divided into groups of 3, collecting the modal displacements of each considered mode, still referring to the global 3D reference system. The total number of columns is variable and

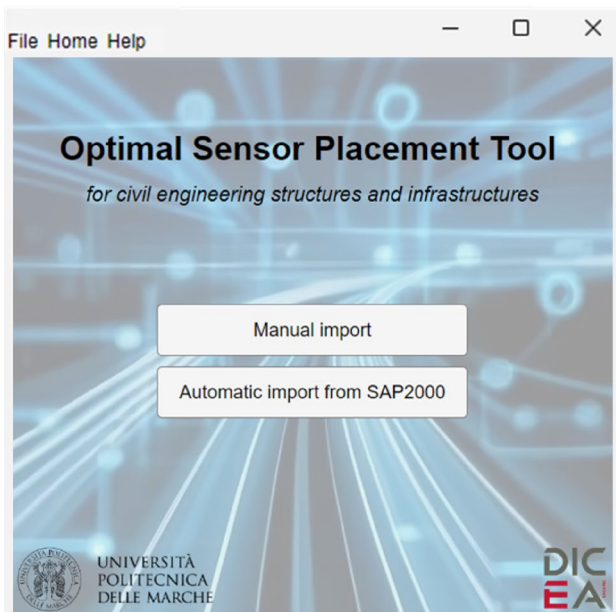


Fig. 1 Graphical user interface (GUI) of the OSP software

Fig. 2 Standard tables for the manual import option: **a** modal displacement input table, **b** frequency input table

Modal Displacements Input									Frequencies Input
Joint name	Angle	X	Y	Z	X_i	Y_i	Z_i	...	Frequency [Hz]
(a)									(b)
									i -th mode frequency

Candidate joint global coordinates
 i th mode shape displacement components

depends on the number of vibration modes to be considered in the OSP analysis. The second table (Fig. 2b) is very simple and consists of a single column vector collecting frequencies of the considered modes in the previous table.

The automatic import from SAP2000 supports the development of the OSP analysis on numerical models and requires preliminary steps to be completed within this commercial software. First, candidate joints considered in the OSP analysis have to be assigned to a dedicated group. If the complete structure has different orientations in its component blocks, separate groups must be created for each section of the building with a local reference system differently oriented from the global one. Then, in the proposed OSP software (left-hand side of the automatic import part of Fig. 3), the SAP version on the workstation have to be set in. After that, by clicking on the “Load” button, the software automatically opens the SAP2000 software and load the numerical model of the structure to be analyzed.

At that point, the user has to define the load condition on which the modal displacements are determined (“Load Case”, generally modal analysis), the maximum number of modes to be obtained from the modal analysis (“Max modes”), the modes among them to be used for the OSP (“Modes”), and the joint groups to be considered. Pressing the “Run SAP” button, the software starts the analysis in SAP2000 and extracts the necessary input data for OSP. Finally, the circle icon becomes green, and the user can click the “View” button to check the correctness of the data extracted from SAP2000.

The right-hand side of the input part of Fig. 3 is used to perform the OSP analysis and it is common to both the input modalities (manual and automatic). Here the user has to define the number of modes (“N. Modes”) and sensors (“N. Sensors”) to be considered in the monitoring system development. The former indicates which modes are considered in the OSP procedure with the target to be clearly identifiable by the obtained sensor configuration. The user can load many modes into the software, but only the first “N. Modes” are considered and used for the OSP analysis. The number of sensors is a constraint for the analysis, and it is commonly based on practical considerations, including available funding and the performance of the acquisition

system and measurement chain. However, this number should not be lower than the number of modes to be identified (“N. Modes”) to avoid spatial aliasing issues. Also, the user has to define the maximum number of sensors (“Max N. Sensors”). This is used to calculate metrics and to investigate the appropriate number of sensors to be deployed, as it will be explained in more detail later. So, generally, this number is much larger than “N. Sensors”. Lastly, the OSP method to perform is selected and the OSP analysis is run by clicking the “Run” button. The user can select multiple OSP methods by checking the box next to each method name; also, all methods can be simultaneously run. By clicking the “Metrics” button, a figure illustrating the graphs of the two metrics discussed in Sect. 2 appears, as shown in the next examples.

Results are displayed in the Results panel (Results Section of Fig. 3) by selecting the method to display with the drop-down menu. Results are organized in a table, with the first column listing the names and directions of the selected joints, and the next 3 columns displaying their global coordinates. For each method, the values of the two metrics calculated by considering the minimum number of sensors (“N. Sensors”) are also stated. Clicking the “Plot” button generates a graphical representation of the results for the selected method, with the possibility to navigate through the figure. Result tables can be saved as .xlsx files using the “Save” button. A flowchart detailing the software architecture and how it can be used is reported in Fig. 4.

The OSP methods implemented in the software identify optimal sensor locations independently of the chosen mode shape normalization (mass or displacement). Since sensor placement depends only on the shape, results remain consistent with the selected normalization strategy, though the software itself does not perform normalization.

4 The novel OSP software validation through simple structural elements

The novel OSP software validation is performed by using two simple numerical examples modelled in SAP2000: a simply supported 2-span beam (Fig. 5a) and a 4-edge fixed

Fig. 3 Main software screens and display of results

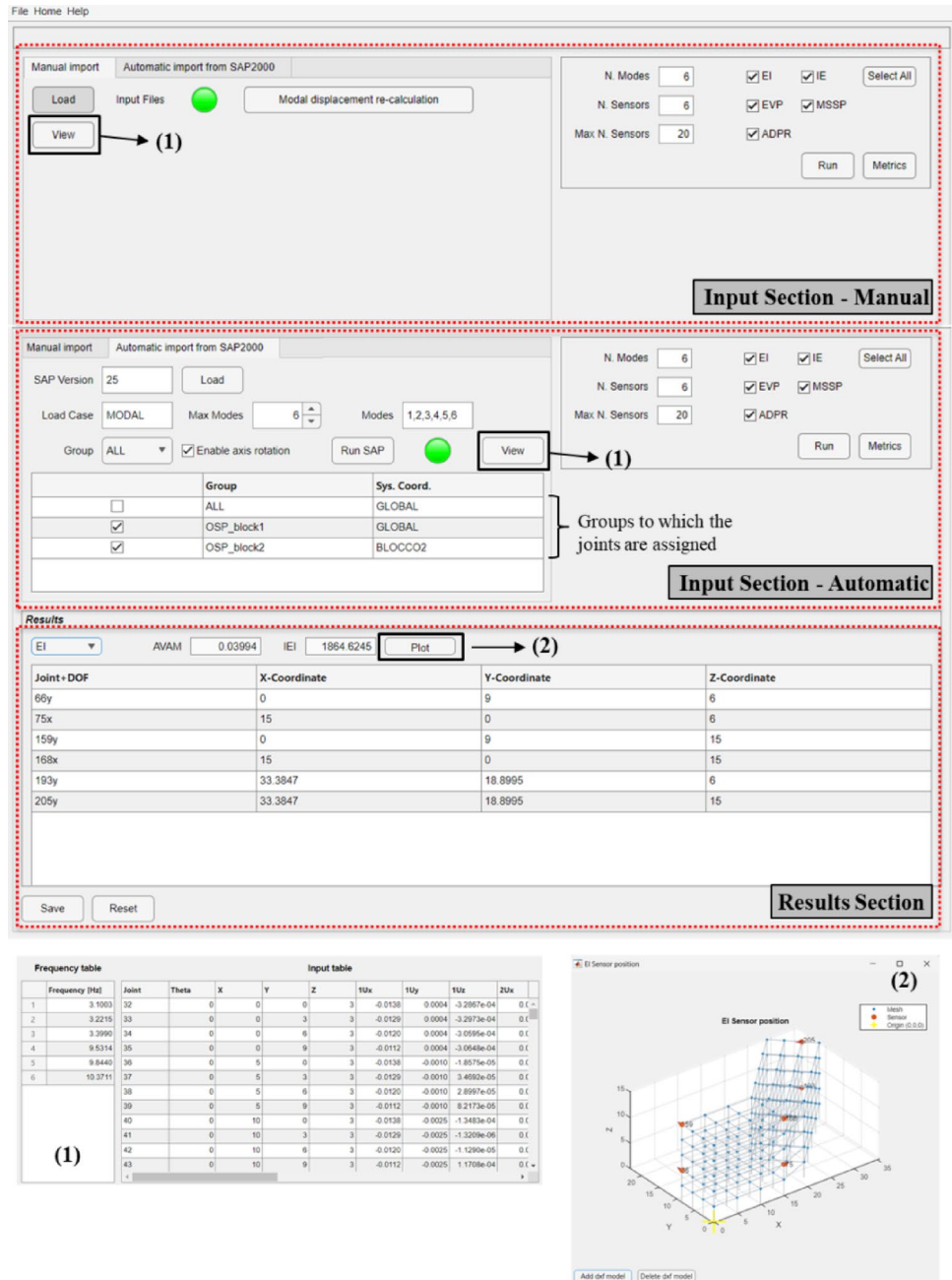


plate (Fig. 5b). Two simple examples are used to better understand and control the sensor configurations provided by the software. The beam model is discretized into 40 beam elements with the same length and 41 joints, 39 of them free to move vertically, along the global Z axis. The latter are considered as candidate joints to detect the vertical (Z axis) modal behaviour of the simply supported beam. The fixed plate is discretized into 375 square shell elements, for a total number of joints equal to 416, 336 of them are free to move vertically (Out-Of-Plane – OOP). Hence, to investigate the OOP dynamic behaviour of the plate, the 336 candidate joints are considered. Being both models

developed in SAP2000, the automatic import option of the novel OSP software is used. The selected modes for the OSP are the first 6 for both the structures. Consequently, a minimum number of sensors equal to 6 is considered. Moreover, a higher maximum number of sensors (20 sensors) is defined for both examples to investigate the best number of sensors to employ in their dynamic SHM by analyzing the metric evolutions. It is worth highlighting that for all the presented case studies (also the real structures in the sequel), the mass-normalization approach for mode shape representation is used.

Fig. 4 Flowchart describing the software architecture and use

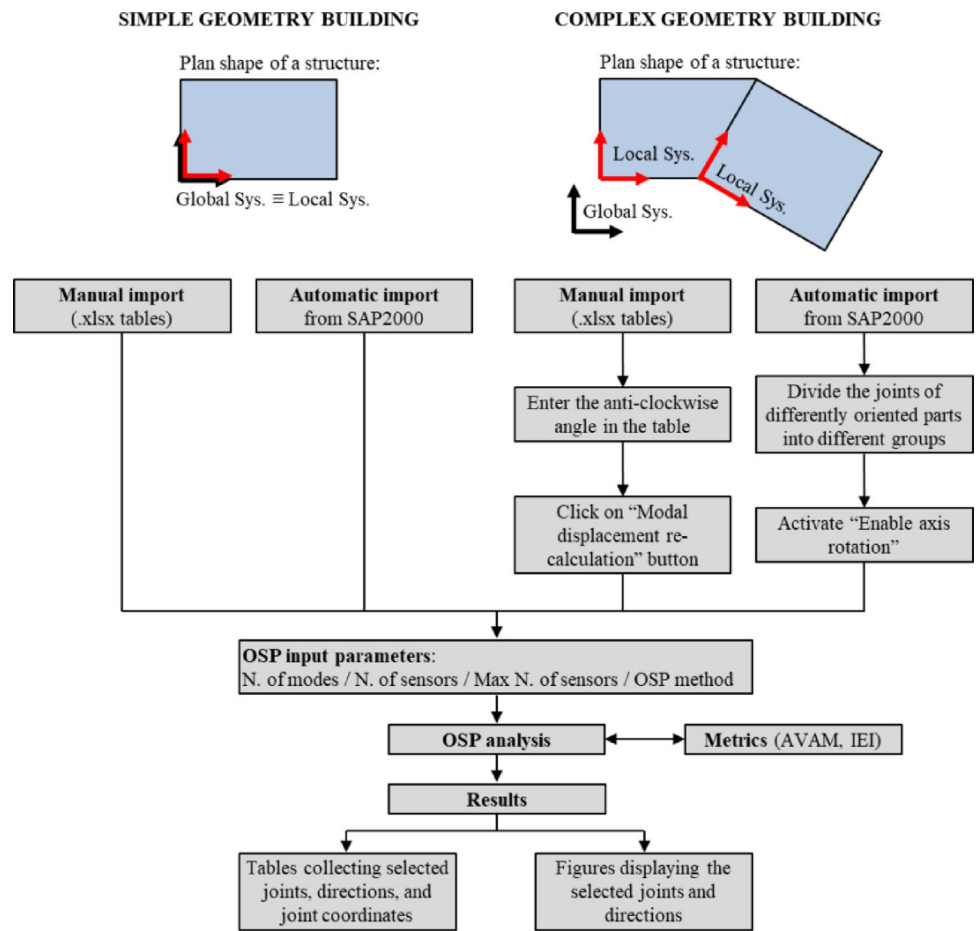
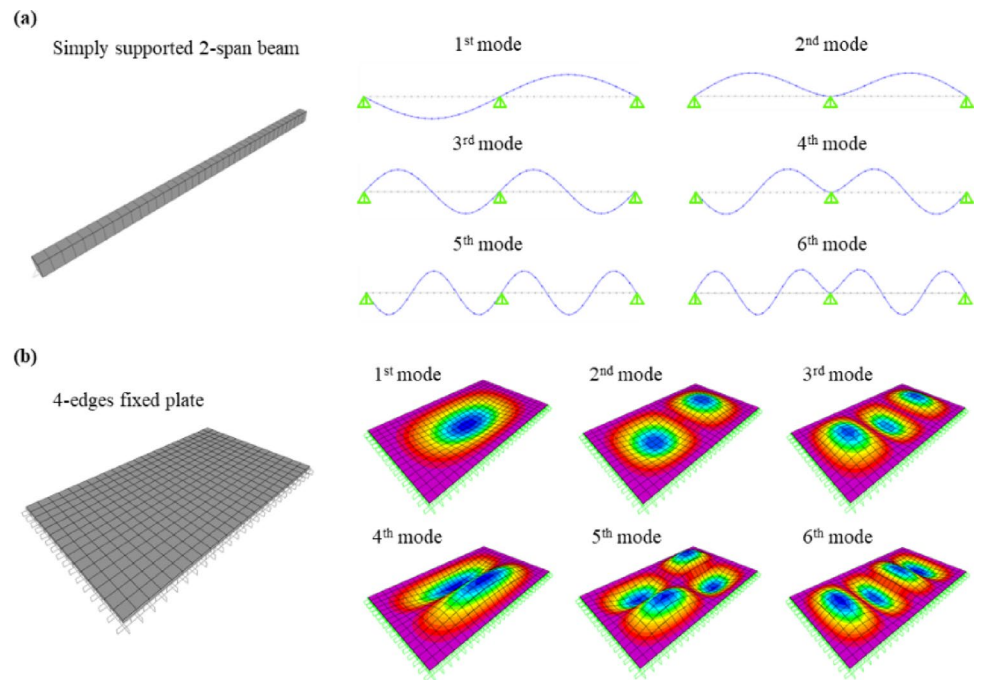


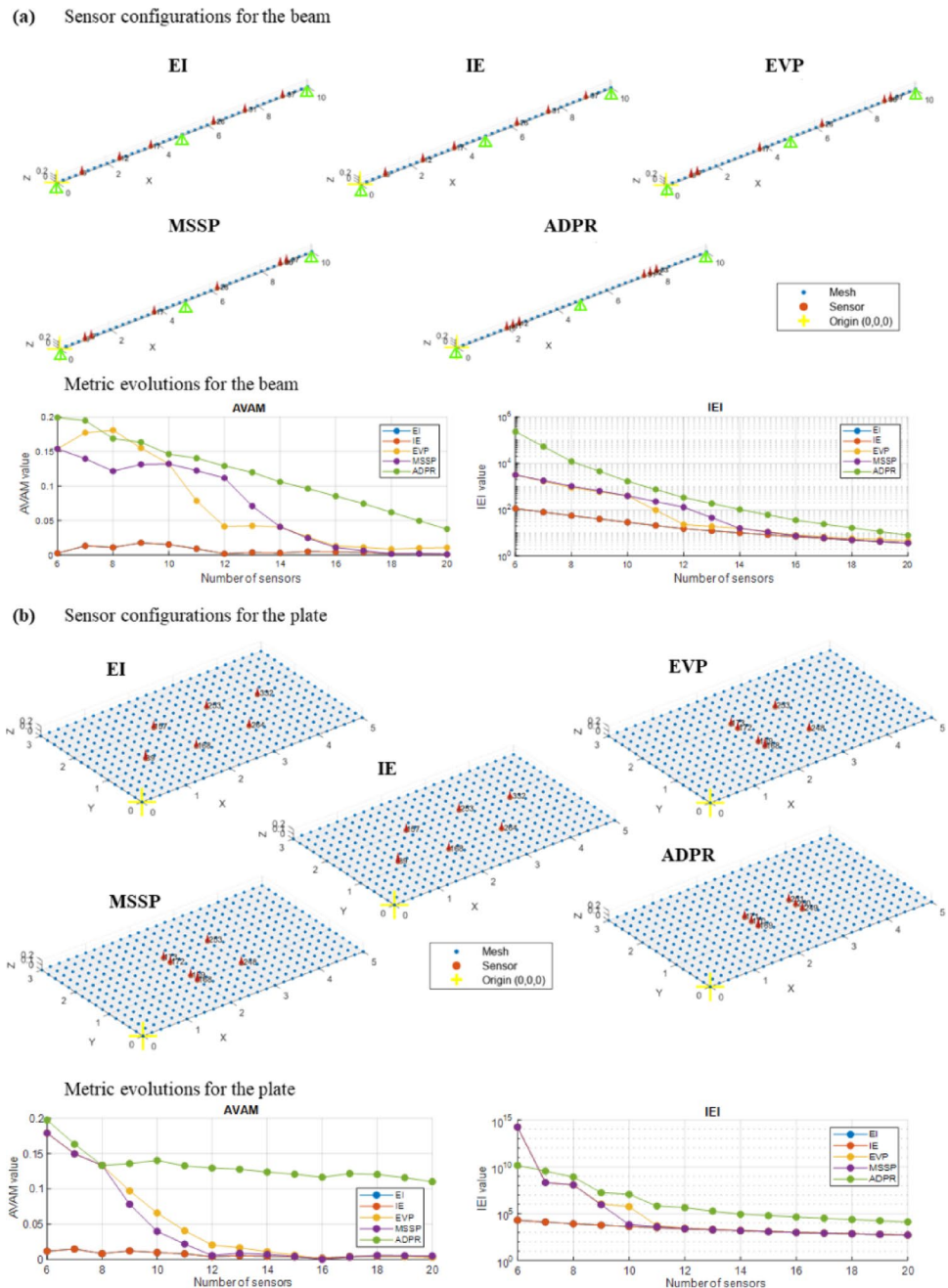
Fig. 5 Simple numerical models for the novel OSP software validation: **a** a simply supported 2-span beam, **b** 4-edges fixed plate



Results of the OSP analyses performed with the novel OSP software are reported in Fig. 6. These figures are obtained from the software by pushing the “Plot” button in the Results section. All the selected joints are displayed with red arrows, indicating the measurement direction (i.e., the selected DOF). Starting from the beam (Fig. 6a), the EI and IE methods result in an identical sensor configuration, with 6 sensors spread all along the entire length of the beam. These configurations are suitable for well capturing all the 6 considered vibration modes without falling in spatial aliasing issues. The EVP and MSSP methods produce identical configurations; however, unlike before, sensors

are concentrated in four positions and it is no longer possible to distinguish the mode shapes between the 1st and 5th modes, as well as between the 2nd and 6th. Finally, the ADPR method concentrates all sensors at the mid-length of each span of the beam, highlighting its ability in well capturing the mode shapes of the first vibration modes (in this case, the 1st and 2nd). Similar considerations arise analysing the plate results (Fig. 6b). In fact, also in this case the EI and IE methods provide sensors spread along the plate surface, while the other three methods (EVP, MSSP, and ADPR) tend to concentrate sensors around the centre of the plate, especially the ADPR, focusing on the first mode.

Fig. 6 Results of the OSP analyses on the two simple models from the novel software: **a** beam and **b** plate model



To investigate the ability of the obtained configurations in well capturing all the investigated modes (in terms of mode shape identifiability and orthogonality), the graphs collecting the two metrics can be analysed. These graphs can be opened by pushing the “Metrics” button. By observing the AVAM graph of the beam (whose goal is to achieve zero values), it is possible to assert that with 6 sensors the configurations obtained with the EI and IE methods produce very satisfactory results. Instead, if the EVP and MSSP methods are used, effective sensor configurations can only be achieved when more than 15 or 16 sensors are utilized. If the IEI metric is considered (whose goal is to achieve values equal to 1), this number decreases to 14 sensors. From both metrics it is also clear that an effective sensor configuration is difficult to achieve with the ADPR method, when few sensors are employed, thus allowing this method to be discarded for the determination of the monitoring configuration of the first 6 modes of the beam. For the plate, the EI and IE methods return very good sensor configurations with the minimum number of sensors while, to achieve a satisfactory sensor layout, around 11 sensors have to be employed if the EVP and MSSP methods are used. As before, the ADPR method does not provide an effective sensor layout able to capture the mode shapes of all the considered 6 vibration modes with less than 20 sensors.

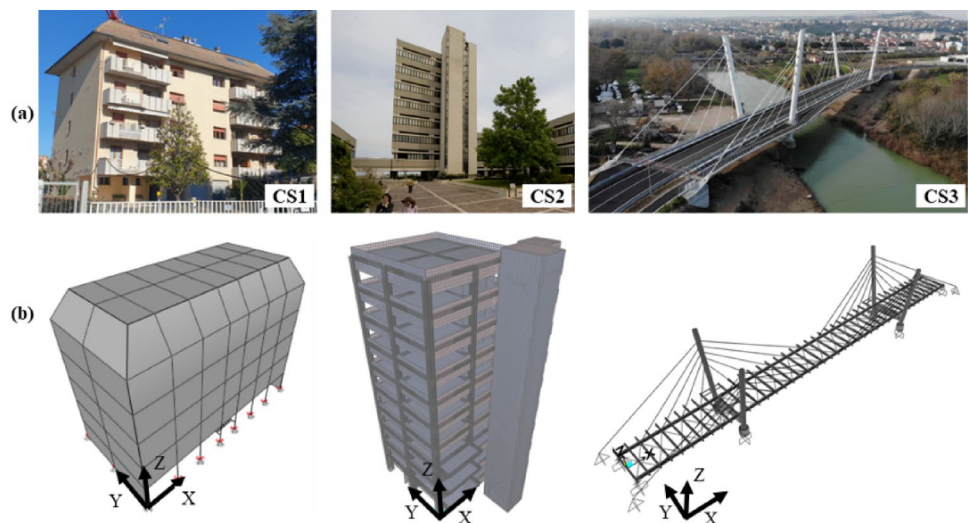
In summary, the new OSP software enables easy and intuitive identification of suitable configurations for dynamically monitoring the two simple structural elements. Additionally, it facilitates precise estimation of the number of sensors needed for their efficient dynamic monitoring.

5 Utilization of the novel OSP software in real case studies

5.1 Description of the case studies

To demonstrate the potentiality of the novel OSP software in supporting the design of dynamic SHM systems, three real case studies are considered. Firstly, they are numerically modelled with Finite Element Models (FEMs), then their dynamic behaviour is used to individuate the best sensor configuration. The case studies represent various structural typologies commonly found in civil engineering. They are a medium-rise residential infilled Reinforced Concrete (RC) building (CS1), a tall building (CS2), and a bridge (CS3). Pictures of the real structures are illustrated in Fig. 7a. CS1 is a residential building with a RC load-bearing structure and masonry infills to build both the interior and exterior walls. It has a compact plan dimension of 11×22 m and 5 elevations above the ground, with a total height of approximately 17 m. The vertical connection is made by an internal staircase with RC bearing structure and a lift. CS2 is the Tower of the Faculty of Engineering located in Ancona (Central Italy). It is a 10-storeys RC frame building with a total height of 50 m and with a square floor plan 9×9 m wide. The tower is flanked by a RC wall structure hosting the stairwell and elevators and separated from the main building with a structural joint. The perimeter walls consist of precast RC panels connected to the beams and disconnected from the columns and strip windows. CS3 is a newly built 3-span cable-stayed bridge constructed over the Saline River in Central Italy. The bridge is 189 m long and the continuous steel-concrete composite deck, supported by 40 diagonal stays, has width ranging from 19.2 to 22.8 m because of the presence of a curved cycle way on the downstream side. The four pylons have total heights of 33.45 and 36.4 m on the upstream and downstream sides, respectively.

Fig. 7 Real case studies: **a** pictures of the RC residential building (CS1), of the Tower of the Faculty of Engineering in Ancona (Italy) (CS2), and of the “Filomena Delli Castelli” bridge in Central Italy (CS3), **b** developed FEMs



5.2 Numerical modelling of the case studies

The FEMs of the case studies are developed by using the SAP2000 software (Fig. 7b). For CS1, the RC frame is modelled by using beam elements, while shell elements are used to model the shear walls of the staircase. Floors are treated as rigid in-plane, with a plane constraint instead of explicit modelling. Vertical roller are applied to the support joints simulating shallow foundations, and rotational and translational springs are introduced in both primary horizontal directions to simulate soil-structure interaction effects and the presence of tie beams. External infill masonry walls are modelled using shell elements, while interior partitions are omitted. CS2 consists of two main parts: the tower structure and the staircase, separated by a structural joint. Frame elements are used for beams and columns, while shell elements for floors, infills, and for the whole staircase. The structure is assumed fixed at the base, as it is supported by deep foundations. The FEM of CS3 is developed by modelling all the steel structural components of the deck and piers with beam elements, except for the stay cables, which are modelled as cable elements. The deck RC slab is not modelled but considered by increasing the stiffness of the main girders; its mass is assigned as a uniform distributed load to the main girders. Pylons are fixed at their base, being founded on piles.

The three FEMs undergo model updating based on detailed ambient vibration tests and operational modal analyses conducted in previous research efforts. For further details on the on-site testing and model updating activities, the reader may refer to [39]. The objective of the updating is to accurately simulate the real dynamic behaviour of the structures. Following this process, the FEMs faithfully capture the actual dynamic characteristics of the real structures. A summary of the dynamic behaviour numerically obtained is reported in Fig. 8; Table 1.

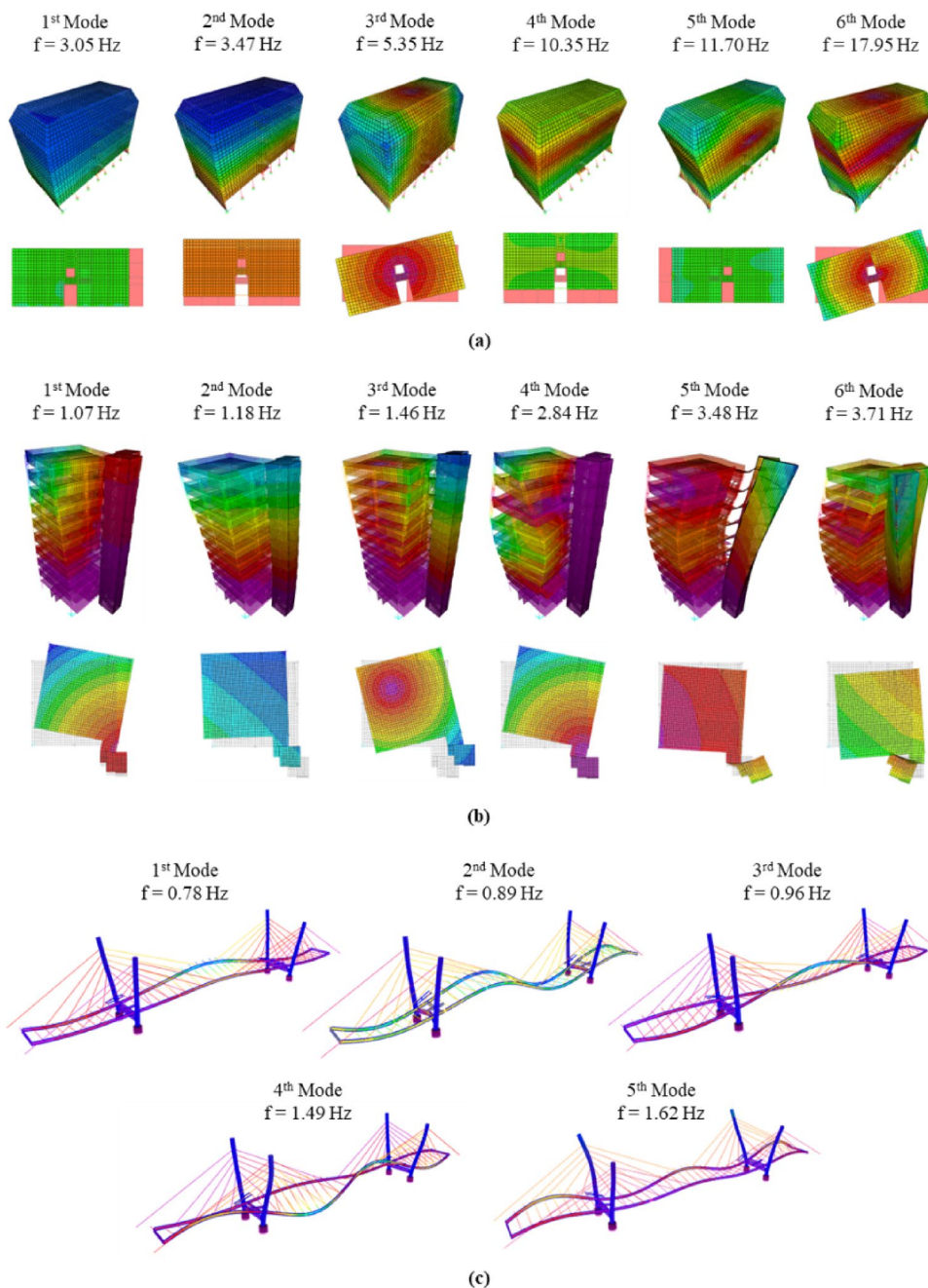
The dynamics of CS1 is characterized by 6 main vibration modes that represent the first and second order longitudinal, transverse, and torsional modes. Also for CS2 the first 6 modes are considered, which represent the first and second order translational and torsional modes. Differently from before, in this case the mode shapes are less clear and intuitive due to the interaction between the main structure and the staircase body, which, although detached with structural joints, is able to influence the dynamics of the entire structure under ambient vibrations. For CS3, the first 5 modes are considered, which represent typical bending and torsional modes of bridge decks also involving the pylons via cables. The vibration modes of each case study reported in Fig. 8 are used as target modes in the subsequent OSP analyses.

5.3 OSP analyses with the novel software

The OSP analyses are separately performed on the three case studies to identify the best sensor configuration to be employed in their dynamic monitoring. It is worth remembering that the main target of an OSP analysis is to find the optimal number and position of sensors that allows the accurate identification of relevant vibration modes to be done, ensuring that the measured signals contain the maximum amount of information and enabling accurate reconstruction of mode shapes. To do so, the input provided to the software are the number of vibration modes to be considered (target modes, the same reported in the previous section), the minimum number of sensors to be employed (equal to the number of target modes), and also the maximum one, the latter useful to investigate the right number of sensors to install (as before, a maximum number of 20 sensors is considered and adopted to plot metric evolutions). The candidate joints for CS1 and CS2 used for the OSP are those of the frame at the intersection between beams and columns, while for the CS3 those at the intersection between the main girders and the transverse beams of the deck. The candidate joints for all case studies are selected based on the ease of sensor installation on the structure. Points that are difficult to access, whether for installation or future maintenance, are excluded from the analyses. For these real applications, the automatic import from SAP2000 option is used; however, exactly the same results are achieved by using the manual import option. All the OSP methods available in the software are used, and the results (software graphical view) and metrics evolutions are reported in Fig. 9. In real case studies, the software allows 3D structure models to be added as backgrounds in sensor position plots by importing .dxf files, ensuring both share the same global coordinate system.

Resulting sensor positions can be briefly discussed as follows. The EI and IE methods distribute sensors all along the structures, allowing for a clear mode shape individuation for all case studies. For CS1 and CS2, sensors at intermediate floors are also suggested, facilitating the individuation of the second order mode shapes, as well as sensors in both the main orthogonal directions of the buildings. The EVP, MSSP, and ADPR methods generally provide configurations with sensors located at the top floor (for CS1 and CS2) or at the mid-span (for CS3), still highlighting their suitability in well capturing the first mode. For CS1 and CS3, the EVP provides a configuration between those obtained with EI and IE (spread sensors) and those obtained with MSSP and ADPR (very concentrated sensors). Observing the metric graphs, it is evident that the considered minimum number of sensors for each case study is enough if the EI and IE methods are considered. Instead, a greater number of sensors is required to achieve a satisfactory configuration

Fig. 8 Vibration modes considered in the OSP procedures: **a** CS1, **b** CS2, **c** CS3



with the other OSP methods. Moreover, for CS2, a sensibly higher number of sensors is required to well capture the mode shapes of the first six modes (around 13–14 with MSSP and ADPR and around 17–18 with EVP).

The analysis of the results confirms that the novel OSP software successfully identified effective sensor configurations in real structures. This demonstrates its suitability for supporting the development of SHM systems in real-world civil engineering applications.

6 OSP of structures with complex geometry and composed by blocks with different orientations

In real world constructions it is common to encounter buildings with complex geometry, namely, with plan shapes composed by different blocks linked together and oriented with diverse angles among them. In cases when these angles are different from 90° (e.g., the structure illustrated in Fig. 10), the decision of sensor positions for the development of a SHM system is not trivial, as well as their orientation. For the sake of simplicity during installation, it is a common

Table 1 Modes considered for each case study for OSP analysis

Structure	Mode	Frequency [Hz]	Mode type (prevalent)
CS1	1	3.05	1st translational mode in X direction (1st longitudinal)
	2	3.47	1st translational mode in Y direction (1st transverse)
	3	5.35	1st torsional mode
	4	10.35	2nd translational mode in Y direction (2nd transverse)
	5	11.70	2nd translational mode in X direction (2nd longitudinal)
	6	17.95	2nd torsional mode
CS2	1	1.07	1st translational mode coupled with torsion
	2	1.18	1st translational mode coupled X, Y directions
	3	1.46	1st torsional mode
	4	2.84	2nd torsional mode
	5	3.48	2nd translational mode coupled X, Y directions
	6	3.71	2nd translational mode coupled X, Y directions
CS3	1	0.78	1st bending mode
	2	0.89	2nd bending mode
	3	0.96	1st torsional mode
	4	1.49	2nd torsional mode
	5	1.62	1st bending mode

practice to place sensors with the principal orientations (x and y axes) equal to those of the part of the building that is instrumented. This notably reduce installation errors, avoiding the use of particular instruments (e.g., compass) or techniques (e.g., trigonometric triangulation) to correctly orient sensors when placed on the structure. If this installation strategy is followed, the OSP analysis must be performed by considering the rotate modal displacements of the block to be monitored instead of the ones referred to the Global Reference System (GRS).

Indeed, as it will demonstrate in the sequel, for a selected mode of the whole complex building, the selected positions after the OSP can be different whether GRS or Local Reference System (LRS) for modal displacement components are considered. This poses another issue about how commercial software return modal analysis results; in fact, they generally provide modal displacements only referred to one reference system, whether global or local, and generally it is hard to have results of the same complex numerical model referred to different coordinate systems. To achieve the latter, the user has to calculate the rotated modal displacements and use them in the OSP software by using the manual import option, but the OSP is time consuming and possible errors may be done.

To solve this issue, the proposed software allows for considering the rotated modal displacement components referred to the LRS of each block once the angles between the GRS and LRS of each block are known. These angles (θ in Fig. 10) are either given by the user (when the manual input option is selected), or automatically recognised by the software (when the automatic import from SAP2000 is done).

For the manual import option, the rotated modal displacements are automatically calculated by the OSP software by clicking on the specific button (“Modal displacement recalculation”), while they are automatically extracted from SAP2000 by activating the “Enable axis rotation” option in the automatic import section. In this second case, the user has to follow few simple steps: on the commercial software SAP2000, the candidate joints of each building block are assigned to a different group, by using the “Assign to Group” command, and a LRS is defined for each block on the basis of its orientation; on the proposed OSP software, each group previously defined is linked to the relevant LRS, by working in the input section (“Sys. Coord.” of Fig. 3).

The rotated components of modal displacements (Φ_r) are calculated by using the following formulae:

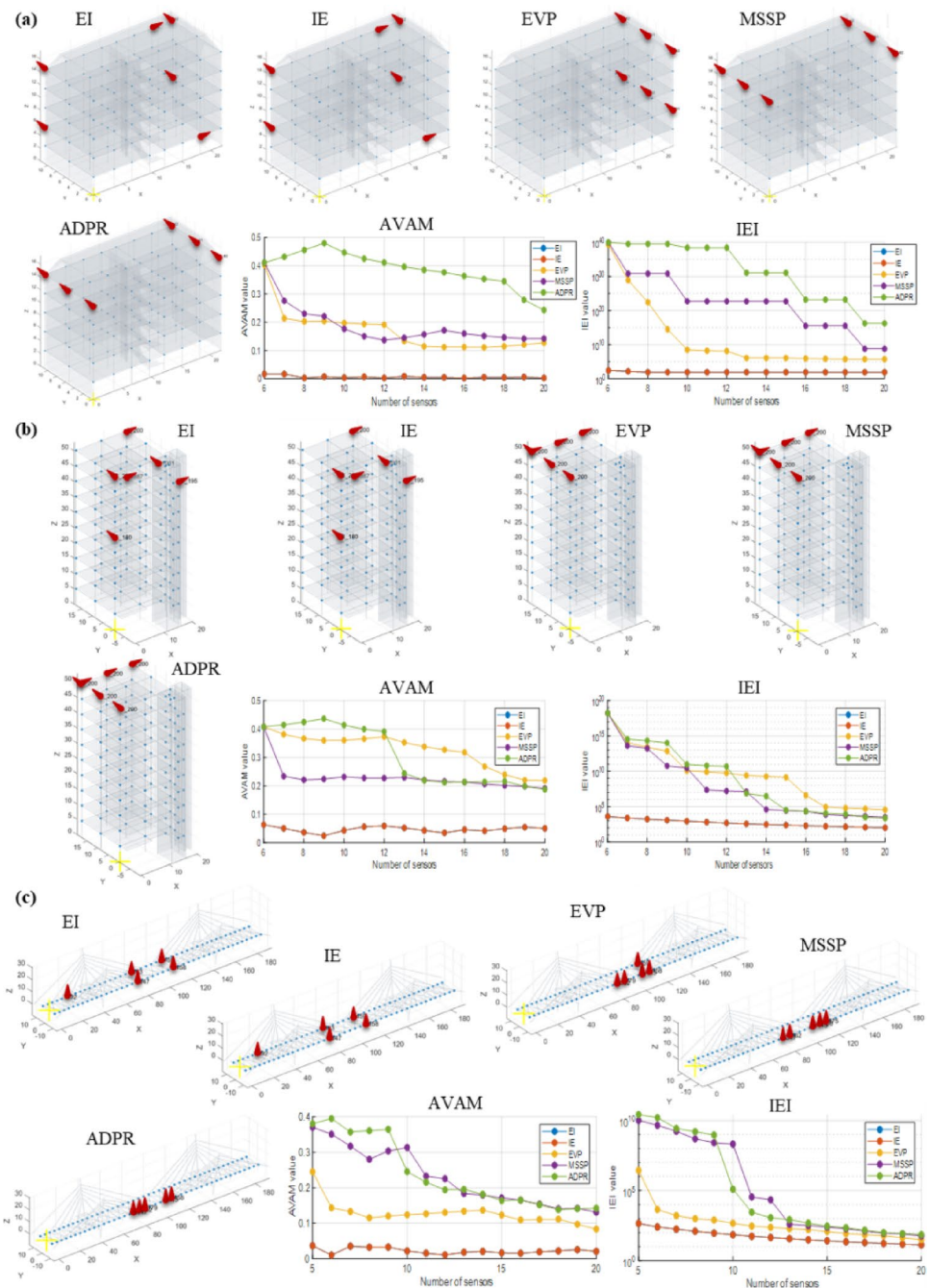
$$\Phi_r = \mathbf{R} \bullet \Phi \quad (11)$$

where Φ is the vector collecting the modal displacements referred to the GRS and \mathbf{R} is the rotation matrix, expressed as follows:

$$\mathbf{R} = \begin{bmatrix} \cos(\theta) & -\sin(\theta) & 0 \\ \sin(\theta) & \cos(\theta) & 0 \\ 0 & 0 & 1 \end{bmatrix} \quad (12)$$

It is worth noting that θ is the anticlockwise LRS rotation angle of each block with respect to the GRS. Once the OSP analysis is performed, the software returns the selected DOFs with reference to the rotated modal displacements, and allows for the plot of these DOFs with rotated arrows oriented along the same principal directions of each block.

Fig. 9 OSP results by using the novel software on the three case studies: **a** CS1, **b** CS2, **c** CS3



To deepen the issue relevant to the OSP of complex buildings with rotated blocks and to show the potentiality of this software option, a numerical application is shown. The examined example refers to the structural frame of a common framed building with residential use and composed by two main blocks rotated each other of an angle $\theta = 45^\circ$ (Fig. 10). Block 1 is composed by 3×3 spans in both x and y directions, with plan dimensions of 15×9 m; Block 2 has four spans in x direction and three in the y one, with plan dimensions of 20×9 m. Both blocks have five floors, for a total height of 15 m. The modal analysis is performed,

and results show that the global dynamics of the structure is characterized by the canonical modes of this type of construction (Fig. 11).

The first three modes are the first longitudinal, transverse, and torsional modes, while the other three are the second longitudinal, second transverse, and second torsional mode. Frequencies are ranging from about 3 to about 10 Hz. It is worth highlighting that the vibration modes are all global modes, denoting modal shapes that contemporary involve both blocks. The OSP analysis is performed by using the automatic import from SAP2000 option and by

Fig. 10 Numerical model of structure with plan shapes composed by different blocks linked together and oriented with diverse angles among them

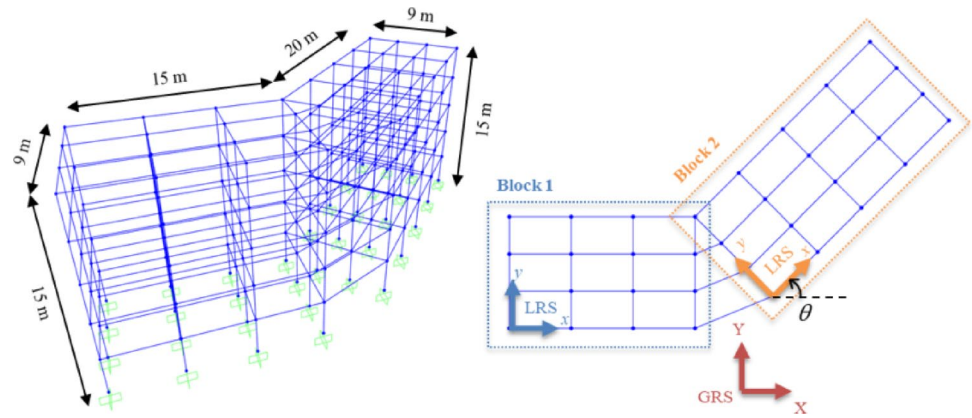
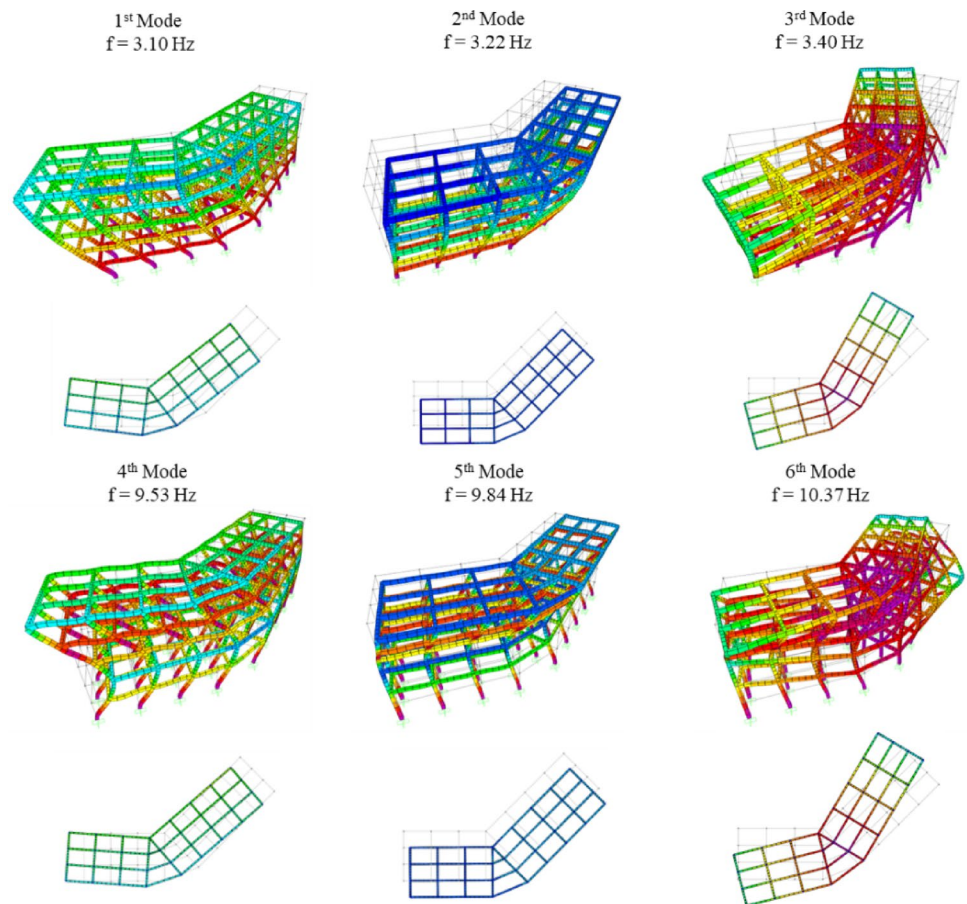


Fig. 11 Target vibration modes for OSP analysis of the example structure with complex geometry and different orientations

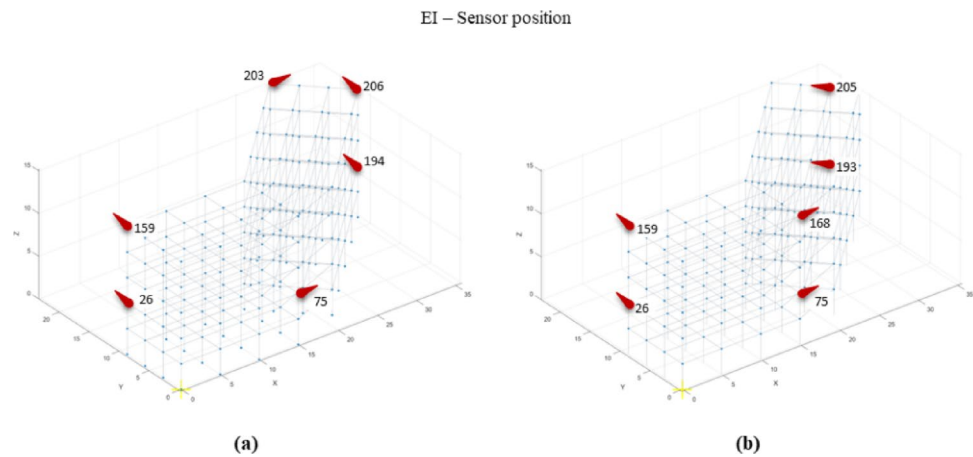


only adopting the EI method, which has been demonstrated to provide better results in terms of sensor distribution over the structure in previous sections. All the 6 vibration modes are considered in the OSP analysis, and the number of sensors is set equal to 6. A former OSP analysis is performed without considering the rotation of the modal displacement components, hence referring for all blocks to the GRS. A second OSP analysis is then performed by enabling the axis rotation and considering the rotated modal displacement components. Results of the two analyses are reported in Fig. 12. For the Block 1, the two analyses select the same

DOFs, while for Block 2 differences are found. When the GRS is considered, 3 DOFs for each block are selected, while, when modal displacements are rotated, only 2 DOFs are selected for Block 2 and 1 DOF moves to Block 1.

To determine which of the two configurations provides better identifiability of the first 6 vibration modes, the two metrics AVAM and IEI are calculated. Considering the non-rotated configuration (GRS), the results are AVAM=0.04 and IEI=8.09 · 10³, whereas for the rotated configuration (LRS), AVAM=0.03 and IEI=1.86 · 10³. The comparison highlights that, in addition to the significant advantage of

Fig. 12 Results of EI method for the example structure with complex geometry and different orientations: **a** results without “Enable axis rotation” option, **b** results with “Enable axis rotation” option



identifying the optimal configuration that allows sensors to be installed orthogonally to the principal directions of each block, the metrics obtained from the rotated configuration are improved.

OSP results highlight the differences in the selection of DOFs in buildings with complex plan shapes, demonstrating the importance of considering the block rotation when sensors are installed along the principal direction of each block.

7 Conclusions

This paper introduced a new software solution for the OSP of civil engineering structures and infrastructures, designed with an intuitive graphical user interface to ensure ease of use. The software streamlines OSP analyses by automating processes, improving efficiency, minimizing human error, and facilitating the creation of robust dynamic monitoring systems for such structures. It integrates five well-established OSP methods, enabling users to determine the optimal number and position of sensors on a structure. Additionally, it supports both numerical and experimental data inputs, with results presented in tabular and graphical formats to clearly illustrate sensor positions. Moreover, it provides two different metric graphs. Tracking metric evolution helps to determine the optimal number and placement of sensors by revealing how sensor configuration performance varies with the number of monitored degrees of freedom.

The novel software architecture and its use was well addressed in Sect. 3. Then, its validation was carried out using simple numerical examples with well-known dynamic behavior (a simply supported 2-span beam and a 4-edges fixed plate), as well as three real case studies. These simple applications demonstrate the ease of interpreting the results and their accuracy in determining the optimal number and position of sensors for the dynamic identification of such structures. The application in real case studies

further demonstrated the effectiveness of the novel software and provided conclusive insights into the suitability of the adopted OSP methods in real civil engineering structures and infrastructures.

A strength and innovation of the proposed software is its capability to conduct OSP analyses on multiple blocks of buildings with complex geometry and with diverse orientations, including non-orthogonal configurations, significantly enhancing its versatility. This approach simplifies sensor installation by aligning their principal orientations with the local axes of each block, minimizing installation errors and removing the need for specialized instruments or techniques. This software potentiality is demonstrated through a numerical example of a 3D frame building with two non-orthogonally oriented blocks. OSP results show that block rotation is crucial for selecting joints and directions in buildings with complex plan shapes. The software could be extended to account for three-dimensional rotations by defining a three-dimensional rotational matrix. This enhancement will be considered in future updates to extend the applicability of the method to more complex civil engineering structures.

The proposed OSP software enhances automated management of structures by enabling real-time monitoring, predictive maintenance, and intelligent response systems. Strategically placed sensors ensure early damage detection, reducing on-site inspections and improving disaster response. By optimizing efficiency, minimizing costs, and ensuring regulatory compliance, OSP facilitates a seamless shift to proactive, data-driven infrastructure management.

Author contributions Conceptualization S.Q., V.N., F.G. - Methodology S.Q., V.N., F.G. - Supervision F.G. - Software S.Q. - Validation S.Q. - Data curation S.Q., V.N. - Visualization S.Q., V.N. - Writing-original draft V.N. - Writing-Review&Editing F.G.

Funding Open access funding provided by Università Politecnica delle Marche within the CRUI-CARE Agreement.

Data availability The authors are willing to provide a trial version of

the software under a temporary license upon reasonable request.

Declarations

conflict of interest The authors have no competing interests to declare that are relevant to the content of this article.

Open Access This article is licensed under a Creative Commons Attribution 4.0 International License, which permits use, sharing, adaptation, distribution and reproduction in any medium or format, as long as you give appropriate credit to the original author(s) and the source, provide a link to the Creative Commons licence, and indicate if changes were made. The images or other third party material in this article are included in the article's Creative Commons licence, unless indicated otherwise in a credit line to the material. If material is not included in the article's Creative Commons licence and your intended use is not permitted by statutory regulation or exceeds the permitted use, you will need to obtain permission directly from the copyright holder. To view a copy of this licence, visit <http://creativecommons.org/licenses/by/4.0/>.

References

- Tran MQ et al (2023) Structural assessment based on vibration measurement test combined with an artificial neural network for the steel truss bridge. *Appl Sci* 13(13):13. <https://doi.org/10.3390/app13137484>
- Ierimonti L, Cavalagli N, Venanzi I, García-Macías E, Ubertini F (2021) A transfer Bayesian learning methodology for structural health monitoring of monumental structures. *Eng Struct* 247:113089. <https://doi.org/10.1016/j.engstruct.2021.113089>
- Tan Y, Zhang L (2020) Computational methodologies for optimal sensor placement in structural health monitoring: a review. *Struct Health Monit* 19(4):1287–1308. <https://doi.org/10.1177/1475921719877579>
- Zhang C, Chun Q, Lin Y (2025) Optimal sensor placement and structural health monitoring methods of ancient stone bridges based on an improved genetic algorithm: taking Lugou Bridge as an example. *Measurement* 241:115680. <https://doi.org/10.1016/j.measurement.2024.115680>
- Hosseini H, Taleai M, Zlatanova S (2023) NSGA-II based optimal Wi-Fi access point placement for indoor positioning: a BIM-based RSS prediction. *Autom Constr* 152:104897. <https://doi.org/10.1016/j.autcon.2023.104897>
- Shin H, Kwak Y (2024) Enhancing digital twin efficiency in indoor environments: virtual sensor-driven optimization of physical sensor combinations. *Autom Constr* 161:105326. <https://doi.org/10.1016/j.autcon.2024.105326>
- Tian K, Gao T, Hu X, Xiao J, Liu Y (2024) Novel optimal sensor placement method towards the high-precision digital twin for complex curved structures. *Int J Solids Struct* 302:113003. <https://doi.org/10.1016/j.ijsolstr.2024.113003>
- Zhong Z, Hua X, Zhai Z, Ma M (2024) A novel tensor-based modal decomposition method for reduced order modeling and optimal sparse sensor placement. *Aerosp Sci Technol* 155:109530. <https://doi.org/10.1016/j.ast.2024.109530>
- Hassani S, Dackermann U (2023) A systematic review of optimization algorithms for structural health monitoring and optimal sensor placement. *Sensors* 23(6):6. <https://doi.org/10.3390/s23063293>
- S. L. Padula and R. K. Kincaid, 'Optimization Strategies for Sensor and Actuator Placement', NASA/TM-1999-209126, Apr. 1999. Accessed: Oct. 14, 2024. [Online]. Available: <https://ntrs.nasa.gov/citations/19990036166>
- Wang Y, Chen Y, Yao Y, Ou J (2023) Advancements in optimal sensor placement for enhanced structural health monitoring: current insights and future prospects. *Buildings* 13(12):12. <https://doi.org/10.3390/buildings13123129>
- Lenticchia E, Ceravolo R, Antonaci P (2018) Sensor placement strategies for the seismic monitoring of complex vaulted structures of the modern architectural heritage. *Shock Vib* 2018(1):3739690. <https://doi.org/10.1155/2018/3739690>
- Zhu K, Gu C, Qiu J, Liu W, Fang C, Li B (2016) Determining the optimal placement of sensors on a concrete arch dam using a quantum genetic algorithm. *J Sens* 2016(1):2567305. <https://doi.org/10.1155/2016/2567305>
- Marano GC, Monti G, Quaranta G (2011) Comparison of different optimum criteria for sensor placement in lattice towers. *Struct Des Tall Spec Build* 20(8):1048–1056. <https://doi.org/10.1002/tal.605>
- Murugan Jaya M, Ceravolo R, Zanotti Fragonara L, Matta E (2020) An optimal sensor placement strategy for reliable expansion of mode shapes under measurement noise and modelling error. *J Sound Vib* 487:115511. <https://doi.org/10.1016/j.jsv.2020.115511>
- Chai W, Yang Y, Yu H, Yang F, Yang Z (2022) Optimal sensor placement of bridge structure based on sensitivity-effective independence method. *IET Circuits Devices Syst* 16(2):125–135. <https://doi.org/10.1049/cds2.12078>
- Cherid D, Bourahla N, Laghoub MS, Mohabeddine A (2022) Sensor number and placement optimization for detection and localization of damage in a suspension bridge using a hybrid ANN-PCA reduced FRF method. *Int J Struct Integr* 13(1):133–149. <https://doi.org/10.1108/IJSI-07-2021-0075>
- Pachón P, Castro R, García-Macías E, Compan V, Puertas E (2018) E. torroja's bridge: tailored experimental setup for SHM of a historical bridge with a reduced number of sensors. *Eng Struct* 162:11–21. <https://doi.org/10.1016/j.engstruct.2018.02.035>
- G. Imposa, A. Barontini, P. B. Lourenco, and S. Russo, 'A Strategy of Optimal Sensor Placement for Dynamic Identification in Cultural Heritage', in *Structural Analysis of Historical Constructions*, Y. Endo and T. Hanazato, Eds., Cham: Springer Nature Switzerland, 2024, pp. 309–321. https://doi.org/10.1007/978-3-031-39603-8_26.
- Civera M, Pecorelli ML, Ceravolo R, Surace C, Zanotti Fragonara L (2021) A multi-objective genetic algorithm strategy for robust optimal sensor placement. *Comput Aided Civ Infrastruct Eng* 36(9):1185–1202. <https://doi.org/10.1111/mice.12646>
- Yi T-H, Li H-N (2012) Methodology developments in sensor placement for health monitoring of civil infrastructures. *Int J Distrib Sens Netw* 8(8):612726. <https://doi.org/10.1155/2012/612726>
- Li DS, Li HN, Fritzen CP (2007) The connection between effective independence and modal kinetic energy methods for sensor placement. *J Sound Vib* 305(4):945–955. <https://doi.org/10.1016/j.jsv.2007.05.004>
- W. E. Hart, J. W. Berry, C. A. Phillips, J.-P. Watson, L. A. Riesen, and R. Murray, 'SPOT: A Sensor Placement Optimization Toolkit for Drinking Water Contaminant Warning System Design.', Sandia National Lab. (SNL-NM), Albuquerque, NM (United States), SAND2007-4393C, Jul. 2007. Accessed: Oct. 14, 2024. [Online]. Available: <https://www.osti.gov/biblio/1147328>
- Arnesano M, Revel GM, Seri F (2016) A tool for the optimal sensor placement to optimize temperature monitoring in large sports spaces. *Autom Constr* 68:223–234. <https://doi.org/10.1016/j.autcon.2016.05.012>

25. Klise K.A., Nicholson B., and Laird C.D., *Sensor Placement Optimization using Chama*. (2017). SANDIA, Albuquerque, New Mexico.
26. J. Dong, L. Zhu, Y. Liu, and D. T. Rizy, (2019) 'Enhancing Distribution System Monitoring and Resiliency: A Sensor Placement Optimization Tool (SPOT)', in *2019 IEEE Power & Energy Society General Meeting (PESGM)*, pp. 1–5. <https://doi.org/10.1109/PESGM40551.2019.8973635>.
27. Tang L, Saxena A, Evans S, Iyer N, Goldfarb H (2023) OSPtk: cost-aware optimal sensor placement toolkit enabling design-for-phm in critical industrial systems. *Annu Conf PHM Soc* 15:1. <https://doi.org/10.36001/phmconf.2023.v15i1.3557>
28. Yi T-H, Li H-N, Gu M (2011) Optimal sensor placement for structural health monitoring based on multiple optimization strategies. *Struct Des Tall Spec Build* 20(7):881–900. <https://doi.org/10.1002/tal.712>
29. Wu ZY, Zhou K, Shenton HW, Chajes MJ (2019) Development of sensor placement optimization tool and application to large-span cable-stayed bridge. *J Civ Struct Health Monit* 9(1):77–90. <https://doi.org/10.1007/s13349-018-0320-5>
30. Wu ZY, Simpson AR (2001) Competent genetic-evolutionary optimization of water distribution systems. *J Comput Civ Eng* 15(2):89–101. [https://doi.org/10.1061/\(ASCE\)0887-3801\(2001\)15:2\(89\)](https://doi.org/10.1061/(ASCE)0887-3801(2001)15:2(89))
31. Mahjoubi S, Barhemat R, Bao Y (2020) Optimal placement of tri-axial accelerometers using hypotrochoid spiral optimization algorithm for automated monitoring of high-rise buildings. *Autom Constr* 118:103273. <https://doi.org/10.1016/j.autcon.2020.103273>
32. Kaveh A, Mahjoubi S (2019) Hypotrochoid spiral optimization approach for sizing and layout optimization of truss structures with multiple frequency constraints. *Eng Comput* 35(4):1443–1462. <https://doi.org/10.1007/s00366-018-0675-6>
33. Kammer DC (1991) Sensor placement for on-orbit modal identification and correlation of large space structures. *J Guid Control Dyn* 14(2):251–259. <https://doi.org/10.2514/3.20635>
34. Papadimitriou C (2004) Optimal sensor placement methodology for parametric identification of structural systems. *J Sound Vib* 278(4):923–947. <https://doi.org/10.1016/j.jsv.2003.10.063>
35. C. B. Larson, D. C. Zimmerman, and E. L. Marek, (1994) 'A Comparison of Modal Test Planning Techniques: Excitation and Sensor Placement Using the NASA 8-bay Truss', vol. 2251, p. 205
36. J. P. DeClerck and Avitabile, P., (1996) 'Development of several new tools for modal pre-test evaluation', in *14th International Modal Analysis Conference (IMAC)*, in 1272, vol. 2768
37. Leuven Measurement Systems (LMS International), 'Large-scale modal testing of a space frame structure from pretest analysis to FEA model validation'. 1991.
38. Nicoletti V, Quarchioni S, Amico L, Gara F (2024) Assessment of different optimal sensor placement methods for dynamic monitoring of civil structures and infrastructures. *Struct Infrastruct Eng*. <https://doi.org/10.1080/15732479.2024.2383299>
39. Amico L, Nicoletti V, Martini R, Carbonari S, Gara F (2025) Impact of combined seismic and energy renovation works on the dynamics and damageability of infilled RC frame buildings. *J Build Eng* 104:112169. <https://doi.org/10.1016/j.jobbe.2025.112169>

Publisher's Note Springer Nature remains neutral with regard to jurisdictional claims in published maps and institutional affiliations.